Biophysical Chemistry 137 (2008) 43–48

Contents lists available at ScienceDirect

Biophysical Chemistry

journal homepage: http://www.elsevier.com/locate/biophyschem

Secondary structure conversions of *Mycobacterium tuberculosis* ribonucleotide reductase protein R2 under varying pH and temperature conditions

Elka R. Georgieva [a,*,1], Ana Julia Narvaez [a,2], Niklas Hedin [b], Astrid Gräslund [a]

[a] Department of Biochemistry and Biophysics, Stockholm University, Arrhenius Laboratories for Natural Sciences, Svante Arrhenius väg 10-12, S-10691 Stockholm, Sweden
[b] Department of Physical, Inorganic, and Structural Chemistry, Stockholm University, Arrhenius Laboratories for Natural Sciences, Svante Arrhenius väg 10-12, S-10691 Stockholm, Sweden

ARTICLE INFO

Article history:
Received 20 April 2008
Received in revised form 23 June 2008
Accepted 23 June 2008
Available online 27 June 2008

Keywords:
Mtb RNR R2 protein
CD spectroscopy
DLS
Aggregation
Molten globule
pH dependence

ABSTRACT

The structural properties of *Mycobacterium tuberculosis* (Mtb) ribonucleotide reductase R2 protein were studied under varying pH and temperature conditions by circular dichroism (CD) spectroscopy as well as dynamic light scattering (DLS). Under physiological conditions this protein has a high α-helical content, similar to the corresponding protein from other species, e.g. mouse. Decreasing the pH induced significant structure conversions. When pH was below 6.5 an aggregated structure was observed and reached a maximum at pH 4. The aggregated state of this protein was verified by DLS and was found to be rich in β-structure. This amyloid-like structure transformed into a molten globule state with high temperature stability (between 25 and 80 °C) at pH below 3. The corresponding mouse protein R2 under similar conditions showed no evidence of an aggregated state around pH 4.

1. Introduction

Ribonucleotide reductase (RNR) are enzymes responsible for providing the deoxyribonucleotide precursors for DNA replication and repair in all DNA-dependent organisms. Three separate classes of ribonucleotide reductases are known: Class I — O_2 dependent, class II — O_2 independent and class III — O_2 inhibited. Class I enzymes are composed of the two homodimeric proteins R1 and R2, generally in an $\alpha_2\beta 2$ configuration. Two subclasses Ia and Ib have been distinguished, based on sequence similarities and allosteric regulation properties. Class Ia is found in mammalian cells and certain bacteria such as *E. coli*, whereas class Ib is common for most bacteria. Protein R1 has the substrate binding site, whereas R2 has a stable free radical on a tyrosine residue, neighboring an antiferromagnetically coupled high spin Fe(III)–Fe(III) site [1–5] in each polypeptide of the R2 dimer. The radical/diiron site is necessary for the enzyme activity. Recent reports show that a stable manganese(IV)/iron(III) cofactor is responsible for the RNR activity in *Chlamydia trachomatis* functioning without a tyrosyl radical, thus giving rise to a new RNR subclass Ic [6–8].

The *Mycobacterium tuberculosis* (Mtb) RNR belongs to subclass Ib [5,9]. Two genes encoding the small RNR subunit denoted R2-1 and R2-2 respectively have been characterized [10]. The R2-2 is generally the enzymatically active form. Reactivity studies as well as data, characterizing the tyrosyl radical and diiron site in Mtb RNR have been reported [11–13].

Earlier studies on RNRs concern predominantly the properties of the tyrosyl radical and the metal site, which are responsible for the catalytic function of these enzymes [1,3–6,14–18]. The structural properties of several RNR enzymes have been characterized by X-ray crystallography, generally of proteins R1 and R2 separately. Secondary structures of the proteins in the solution state have also been studied by CD spectroscopy. For *E. coli*, mouse, yeast and Mtb R2 proteins at ambient conditions [19–21] the secondary structure is predominantly α-helical for R2 proteins under these conditions, also in agreement with the crystal structures.

Here we have explored pH and temperature dependent secondary structure variations of Mtb R2 and compare with the results from mouse R2 protein, which has a very similar three-dimensional structure in the native state. We have used circular dichroism (CD) and dynamic light scattering (DLS) to characterize the structural states. Interestingly we find evidence of wide structural variations for MtbR2, involving both aggregation and concomitant conversion to β-structure, as well as further conversion to a molten globule-like structure as the pH is lowered from pH 7 to pH 2. This is in contrast to the behavior of mouse R2, which displays no intermediate aggregated structure.

* Corresponding author. Tel.: +1 607 255 6132; fax: +1 607 255 6969.
E-mail address: erg54@cornell.edu (E.R. Georgieva).
[1] Current address: Baker Laboratory, Department of Chemistry and Chemical Biology, Cornell University, Ithaca, NY 14853-1301, USA.
[2] Current address: Department of Oncology, University of Cambridge, Hutchison/MRC Research Centre, Box 197 Hills Road, Cambridge CB2 0XY, UK.

0301-4622/$ – see front matter © 2008 Elsevier B.V. All rights reserved.
doi:10.1016/j.bpc.2008.06.009

2. Experimental

2.1. Expression and purification of native R2 proteins

Mtb R2-2 and mouse R2 proteins were overexpressed in logarithmically growing Rosetta 2(DE3)pLysS bacteria containing pETR2 plasmids encoding native Mtb and mouse R2 proteins. For expression of both R2 proteins, an overnight culture of Rosetta 2(DE3) pLysS inoculated with Mtb R2 was diluted 200 times in 4.8 l of Luria-Bertani medium, containing 34 mg/ml of chloramphenicol and 100 mg/ml of carbenicillin. The bacteria were grown at 37 °C until they reached an A_{595} of 0.6–0.8 and then induced with 400 mM Isopropyl beta-D-1-thiogalactopyranoside and grown for additional 18 h at 14 °C before harvesting. The mouse R2 protein was purified using the protocol described in Narvaez et al. [15]. For Mtb R2-2 protein purification the same protocol was used with small modifications during the chromatographic step. Two washing steps were applied using a 10 mM phosphate buffer with 80 mM and 150 mM KCl, respectively, to wash the protein. The protein was then eluted using a 10 mM phosphate buffer with 230 mM KCl.

All procedures during the protein extraction and purification were done at 4 °C or on ice. Protein concentration was determined as previously described [20,22].

2.2. Sample preparation

Both R2 proteins were in 50 mM Tris buffer–HCl, pH 7.4 at room temperature (RT). From now on the term "normal medium" will be used for samples in this buffer. The desired pH was achieved by adding appropriate amounts of 1 M HCl or NH_3 in water. The pH was measured by a pH meter ORION, mode 320. It was not possible to measure pH of samples with very high acid/base concentration and in the text below we will mention their concentrations, not pH. R2 concentration in the text refers to the molar concentration of R2 polypeptide.

2.3. Circular dichroism (CD) spectroscopy

CD spectra were recorded in the far-UV range between 190 and 250 nm in the temperature interval between 4 and 100 °C on a Jasco J-720 Spectropolarimeter by using a quartz cells with a 0.1 and 0.2 mm optical path length. The scanning speed was 100 nm/min, bandwidth — 2 nm and resolution — 0.5 nm.

Samples of Mtb R2 with polypeptide concentration of 17 and 2 μM and pH between 12 and 2 as well as samples with the same polypeptide concentration and very high HCl or NH_3 concentrations (up to 200 mM) were used. Samples of mouse R2 with polypeptide concentration of 17 μM and pH between 7.4 and 2 as well as a sample with the same polypeptide concentration and HCl concentration of 200 mM were investigated. For the pH dependence measurement, samples were stored at 25 °C for 15 min and then measured at the same temperature. For the temperature dependence measurement, samples of 17 μM Mtb or mouse R2 polypeptide in "normal medium" or low pH medium were prepared at room temperature (RT, about 25 °C), stored at 25 °C for 15 min and measured at gradually increased temperatures. The time for temperature stabilization between every two measurements was 5 min. All CD spectra were baseline corrected, using a spectrum of 50 mM Tris–HCl buffer, pH 7.4 at RT.

The theoretical analysis of CD spectra was performed by the DicroWeb program, analysis program — CDSSTR, reference set 7, with input and output data in mean residue ellipticity units [23,24]. The mean residue ellipticity was calculated by using a manufactured program and the number of the amino acids residues R2 polypeptide was taken from a protein database. The results were obtained in terms of the secondary structures introduced in Sreema et al. [25]. The authors define α-helices and β-strands as divided into two classes, corresponding to regular and distorted helices and strands, respectively, and in addition turns, and unordered structures. Here we have grouped the different structures into three distinguishable classes — a sum of both types of α-helices, a sum of both β-structures and turns, and disordered structure.

2.4. Dynamic light scattering (DLS)

DLS was used for the protein particle size determination. The measurements were performed on a Zetasizer Nano ZS Malvern Instrument. The signal/noise was automatically optimized. The results were presented as volumes distribution. Samples with Mtb R2 polypeptide concentrations of 17 μM were used. The range of pH was between 7.5 and 2. For the pH dependence measurement, samples were stored at 25 °C for 15 min and then measured at the same temperature. All CD and DLS measurements were performed three times, either on the same sample or on three similar samples.

2.5. Light absorption spectroscopy

Electronic spectra were recorded on a Jasco V-560 UV/VIS spectrophotometer at room temperature. A cell with 1 cm path length was used. The band width was 2 nm, the scanning speed was 100 nm/min, and the data pitch was 1 nm. Samples with Mtb R2 polypeptide concentration of 100 μM in media with pH between 7.4 and 2 were measured.

2.6. Amino acid sequences analysis

Mtb and mouse RNR R2 protein sequences were taken from the NCBI databases [26] and the analysis including amino acid sequences identity/similarity or hydrophobicity was done using EMBOSS Pairwise alignment algorithms or Mobyle program for bioinformatics analyses [27,28].

3. Results

Circular dichroism (CD) and dynamic light scattering (DLS) have been used to characterize secondary structures under varying experimental conditions in Mtb and mouse R2 proteins from RNR. Both proteins are homodimers with molecular weights of 2×36 991 Da and 2×45 095 Da, respectively, with 324 or 390 residues per monomer.

3.1. Light absorption spectroscopy

The absorbance between 300 and 700 nm of the diiron cluster and free radical of Mtb R2 was studied at varying pHs (data not shown). At pH 7.4 the spectrum showed the typical features of native R2, similar to those presented in Liu et al. [20]. At pH below 6.6 and down to pH below 4 the spectrum was dominated by light scattering. However, at pH 2 the light absorption of a typical protein without the diiron/radical cluster was observed. The pH dependence of light absorption

Table 1
Secondary structures evaluated for Mtb R2 protein in aqueous solvents with different pH — results from CD spectra calculations with the DichroWeb program

pH	*Helices, %*	*β-structures, %*	*Unordered, %*
7.4	89	6	4
6.77	82	14	5
5.97	90	6	3
4.65	33	39	30
3.97	41	36	22
3.22	78	12	9
2.36	67	21	11
2	63	21	16

Experimental conditions: 25 °C measurement temperature, R2 polypeptide concentration — 17 μM.

Table 2
Secondary structures evaluated for mouse R2 protein in aqueous solvents with pH 7.4, 2 or 20 mM HCl — results from CD spectra calculations with DichroWeb program

Sample	*Helices, %*	*β-structure, %*	*Unordered, %*
pH 7.4	66	25	19
pH 2	16	49	34
200 mM HCl	48	34	19

Experimental conditions were: measurement temperature — 25 °C, R2 concentration — 17 μM for polypeptide.

spectrum of Mtb R2 protein initiated a more detailed study of its behavior by other techniques.

3.2. CD spectroscopy and spectra analysis

CD spectra of native Mtb and mouse R2 protein at pH between 7 and 8 showed a dominant α-helical secondary structure with minima in the recorded signal at 208 and 223(4) nm — in general agreement with previously reported spectra for these proteins under similar conditions. A theoretical analysis by the DichroWeb simulation program gave results about the different types of secondary structure, present in the native Mtb and mouse R2 proteins as shown in Tables 1 and 2. In Mtb R2 we calculated 89% of α-helix with very little β-structure and unordered structure. For mouse R2 the corresponding numbers are 66% for the α-helix and 25% and 19% for β-structure and unordered structures, respectively.

The pH dependent conversion of the secondary structures of the R2 proteins was studied in CD experiments using samples containing 17 μM of Mtb and mouse R2 proteins (polypeptide concentration). Spectra were recorded at 25 °C with a path length of 0.1 mm. CD spectra of samples with Mtb R2 protein, recorded in the interval of pH between 7.4 and 2 are shown in Fig. 1. Towards lower pH the Mtb R2 secondary structure undergoes significant changes, characterized by loss of CD intensity and shifts in the CD spectra extremes. Similar experiments for Mtb R2 were repeated on samples with polypeptide concentration of 2 μM, using a quartz cell with 0.2 mm path length. There was no obvious protein concentration dependence when comparing the results for 17 and 2 μM of the R2 polypeptide (data not shown).

Quantitative evaluations of the CD spectra showed a significant loss of CD intensity for Mtb R2 protein in the pH range between 4.7 and 4, accompanied by a relatively high increase of the percentage of β-structure and unordered structures (Table 1). At lower pH, a further secondary structure conversion took place, which gave rise to increased α-helical structures to a percentage almost equivalent to the native one. This high α-helical structure was conserved even at very high acid concentrations in the solvent (up to 200 mM HCl) and no protein precipitation was observed under these conditions (data not shown). Such refolding has been observed for other proteins under different conditions, and has been associated with a molten globule state formation [29–32].

After exposure to the high acid medium the initial CD signal of native Mtb R2 could not be restored by back titration with NH_3. This was investigated using protein samples in a solvent with initially 50 mM HCl. The result indicates that the structure conversion after high acid treatment is irreversible under these conditions. At a pH higher than 7.4 and with very high base concentrations (up to 200 mM NH_3) in the solvent, the secondary structure of the Mtb R2 protein did not change significantly: the evaluated CD spectra showed 66% and 22% for α-helix and β-structure, respectively.

The structural conversions of mouse R2 protein towards low pH were different from those observed for Mtb R2. In the pH interval from 7.5 to 2.6, mouse R2 did not significantly change its secondary structure and no CD intensity loss was observed. At pH 2 and slightly lower than 2, the protein obviously unfolds. For the spectrum recorded at 25 °C (Fig. 2) we calculated 16% of α-helix, 49% of β-structure and 34% of unordered structure (Table 2). Very high acid concentration in the medium (200 mM HCl) changed the secondary structure of this protein to a somewhat lower percentage of α-helix compared to pH 7.4 (48% related to 66%).

The temperature dependence of the CD spectra of Mtb and mouse R2 protein were studied in “normal medium” and at pH 2. CD spectra were recorded in the temperature interval 25–100 °C, at 5 °C intervals. The CD intensity at 223 nm as a function of temperature is shown in Fig. 3. For Mtb R2 at pH 7.4 the CD intensity shows a transition in the temperature range 65–85 °C, whereas the CD spectra at pH 2 show transitions only above 80 °C. For mouse R2 at pH 7.4, a structure transition was observed between 55 and 65 °C, related to loss of CD

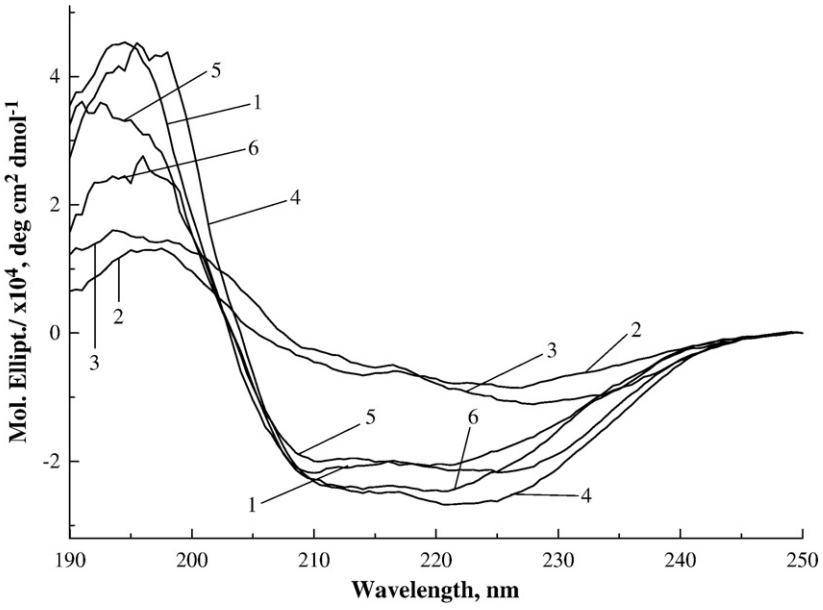

Fig. 1. Far-UV CD spectra of Mtb RNR R2 protein in aqueous solvents with different pH: 1 — pH 6.8, 2 — pH 4.65, 3 — pH 4, 4 — pH 3.2, 5 — pH 2.7 and 6 — pH 2. Spectra measurement temperature was 25 °C, R2 concentration was 17 μM for polypeptide.

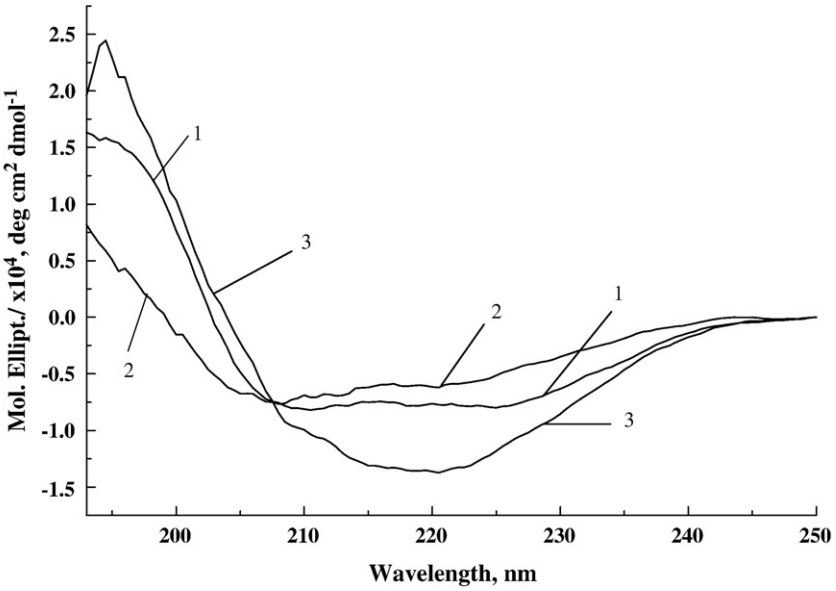

Fig. 2. Far-UV CD spectra of mouse RNR R2 protein in aqueous solvents with different pH: 1 — pH 7; 2 — pH 2; 3 — 200 mM HCl. Spectra measurement temperature was 25 °C, R2 concentration was 17 μM for polypeptide.

intensity at 223 nm and conversion from α-helical to unordered structure (Fig. 3). At pH 2 mouse R2 has predominantly disordered structure, but with a relatively high percentage of β-strands (up to 35%) in the whole temperature range (data not shown).

3.3. Dynamic light scattering

DLS measurements were performed to study pH dependent protein aggregation for the Mtb R2 protein, suggested by the secondary structure transformations and CD intensity loss at pH around 4. Samples contained 17 μM Mtb R2 polypeptide in solvents with pH between 7.4 and 2. From the scattering curves, hydrodynamic radii could be evaluated (Fig. 4). The results showed that the hydrodynamic diameter of the protein particles increases significantly when pH is lowered towards 4 and it goes back to values close to the initial ones at pH 7.4. Three different maxima were observed at pH 6.4 — at 17, 47 and 426 nm suggesting a heterogeneous aggregated state of the protein. Apparently even a moderate decrease of pH from 7.4 to about 6.4 causes aggregation of the Mtb R2 protein. At pH 4 we measured only one peak with a maximum above 2000 nm. Inspection by eye showed that the sample at pH 4 was not optically clear, but whitish and bigger aggregates could be seen. The results at pH 4 suggest that the protein reaches a highly aggregated state, which is shown also by the loss of CD intensity and increased β-structure content (Fig. 1, Table 1). Increase of β-structure accompanied by aggregation is a common designator of amyloid structure [33].

When the pH is further decreased to 2 the protein shows no aggregation. The hydrodynamic diameter (maximum at 10.5 nm) is

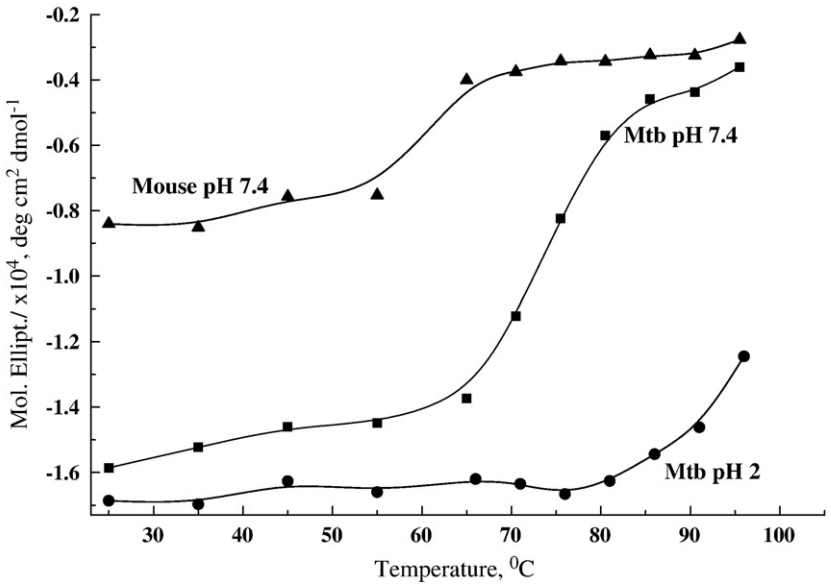

Fig. 3. Plot of CD intensity at 223 nm as a function of the temperature. Samples with Mtb or mouse R2 polypeptide concentration 17 μM, in "normal medium" or in medium with pH 2. Temperature was gradually increased from 25 to 100 °C.

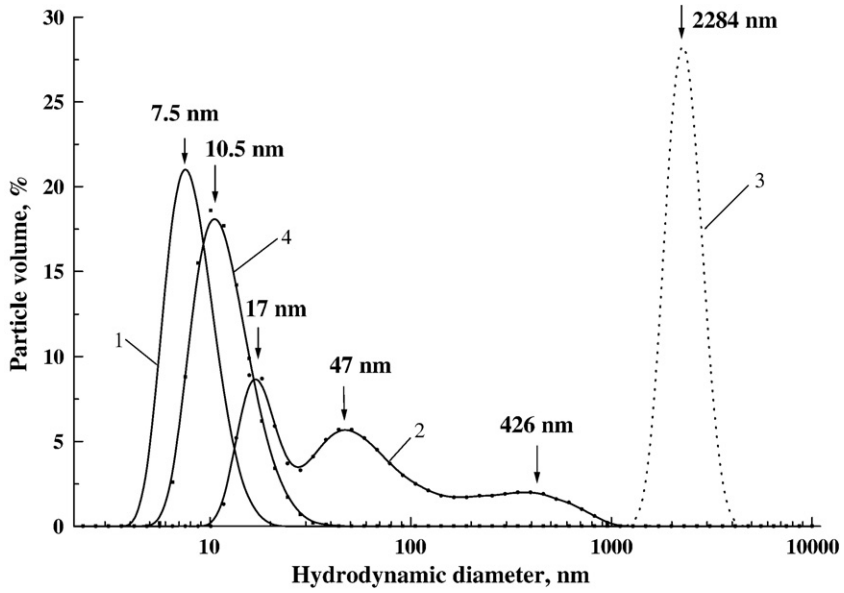

Fig. 4. Plot of DLS results for samples containing 17 μM Mtb R2 polypeptide in aqueous solvents with different pH: 1 — pH 7.4, 2 — pH 6.4, 3 — pH 4 and 4 — pH 2.6. Measurement temperature was 25 °C. Peak maxima are indicated by arrows.

not very different from that of the native protein at pH 7.4 (a maximum at 7.5 nm). The CD spectra showed a considerable amount of the α-helical structure, and the spectra intensities at pHs close to 2 are comparable with those at pH close to 7 (Fig. 1).

Using the equation for hydrodynamic radii suggested by Danielsson et al. [34] for fully unfolded and folded proteins we could calculate expected average values for the hydrodynamic diameter of Mtb R2 molecules to be 14.6 and 6.6 nm, respectively, assuming the protein to be a dimer with a molecular weight of about 75 kDa. Similarly, a prediction using the results of Wilkins et al. [35] for unfolded and native folded proteins after their NMR studies, gave calculated values for the hydrodynamic diameter of 17 and 6.2 nm, respectively. Comparing the calculated values and the experimentally obtained ones we suggest that the increase of hydrodynamic diameter at pH 2 and lower is a result of protein unfolding, without much loss of secondary structure. The experimentally derived diameter for native proteins at pH 7.4 is close to that predicted for folded dimers.

4. Discussion

The present study presents an unexpected structural variability of the Mtb R2 protein, up to now known to be a highly α-helical protein [19]. Around pH 4 the protein exists in a highly aggregated state. The measured hydrodynamic diameter is large compared to the native state and the secondary structure is rich in β-structure. We consider this to be an amyloid-like state. A further decrease of the pH gives rise to a state where the α-helix content is again high and the hydrodynamic diameter is only marginally larger than that of the native protein. This is a molten globule state. The native structure for Mtb R2 at pH 7.4 undergoes a temperature-induced structure conversion around 75 °C, whereas the pH 2 structure is relatively resistant to temperature changes.

It is interesting to note that mouse R2 protein is quite different from Mtb R2 in terms of structure stability and conversions. The two proteins are quite similar in their structural architecture in the native state [26]. They have 17% sequence identity and 33% sequence similarity [27]. Despite these similarities mouse R2 is less temperature stable in its native form, and it is unable to form the amyloid-like structure at pH 4. At pH 2 it is almost completely disordered. Another interesting aspect in our observations is the stability of Mtb R2 molten globule state. A possible explanation may be the high hydrophobicity of this protein — the moles of amino acids per polypeptide with very high and high hydrophobicity are 67% [28]. The corresponding value for mouse R2 is 60% [28]. A study on α-lactalbumin supports this hypothesis [36] — the authors report about mutations to higher hydrophobic residues, which significantly stabilize the molten globule state in this protein. They suggest that the hydrophobic core in a globular protein plays an important role in stabilization of the molten globule state in general.

Behavior similar to that of Mtb R2 has been reported for a number of proteins, for which the ability to aggregate even at ambient conditions is related to amyloid formation and sometimes pathologic phenomena, e.g. in Alzheimer's disease, transmissible spongiform encephalopathies or type II diabetes [37–41]. The present study concerns the pH sensitivity of an analogue of an essential mammalian protein in a pathogenic bacterium. Obviously the energy landscapes of the two proteins, Mtb and mouse R2, are very different, with Mtb R2 exhibiting quite dramatic structure conversions towards lower pH values. The results raise some intriguing questions about whether pH induced aggregation, perhaps promoted by therapeutic intervention, and could be a defense mechanism against an invading pathogen.

Acknowledgments

We thank T. Astlind and B-M. Olsson for the expert technical assistance and Dr. L. Hugonin for the kind help with the CD measurements. This study was supported by the Swedish Research Council (to A. G.) and fellowship from the Carl Trygger Foundation (to E. R. G.).

References

[1] P. Reichard, From RNA to DNA, why so many ribonucleotide reductases? Science 260 (1993) 1773–1777.
[2] B-M. Sjöberg, P. Reichard, A. Gräslund, A. Ehrenberg, The tyrosine free radical in ribonucleotide reductase from *Escherichia coli*, J. Biol. Chem. 252 (1977) 536–541.
[3] L. Petersson, A. Graslund, A. Ehrenberg, B-M. Sjoberg, P. Reichard, The iron center in ribonucleotide reductase from *Escherichia coli*, J. Biol. Chem., 255 (1980) 6706–6712.
[4] A. Jordan, E. Pontis, F. Åslund, U. Hellman, I. Gibert, P. Reichard, The ribonucleotide reductase system of *Lactococcus lactis*. Characterization of an NrdEF enzyme and a new electron transport protein, J. Biol. Chem. 271 (1996) 8779–8785.

[5] M. Fontecave, P. Nordlund, H. Eklund, P. Reichard, The redox centers of ribonucleotide reductase of *Escherichia coli*, Adv. Enzymol. Relat. Areas Mol. Biol. 65 (1992) 147–183.
[6] M. Högbom, P. Stenmark, N. Voevodskaya, G. McClarty, A. Gräslund, P. Nordlund, The radical site in Chlamydial ribonucleotide reductase defines a new R2 subclass, Science 305 (2004) 245–248.
[7] W. Jiang, D. Yun, L. Saleh, E.W. Barr, G. Xing, L.M. Hoffman, M.-A. Maslak, C. Krebs, M. Bollinger Jr., A manganese(IV)/iron(III) cofactor in *Chlamydia trachomatis* ribonucleotide reductase, Science 316 (2007) 1188–1191.
[8] N. Voevodskaya, F. Lendzian, A. Ehrenberg, A. Gräslund, High catalytic activity achieved with a mixed manganese–iron site in protein R2 of *Chlamydia* ribonucleotide reductase, FEBS Lett. 582 (2007) 3351–3355.
[9] F. Yang, G. Lu, H. Rubin, Isolation of ribonucleotide reductase from *Mycobacterium tuberculosis* and cloning, expression, and purification of the large subunit, J. Bacteriol. 176 (1994) 6738–6743.
[10] S.T. Cole, R. Brosch, J. Parkhill, T. Garnier, C. Churecher, D. Harris, S.V. Gordon, K. Eiglmeier, S. Gas, C.E. Barry, F. Tekaia, K. Badcock, D. Basham, D. Brown, T. Chillngworth, R. Connor, R. Davies, K. Devlin, K. Feltwell, S. Gentles, N. Hamlin, S. Holroyd, T. Hornsby, K. Jagels, J. Osborne, M.A. Quail, M.-A. Rajandream, J. Rogers, J.E. Sulson, K. Taylor, S. Whitehead, B.G. Barrel, Deciphering the biology of *Mycobacterium tuberculosis* from the complete genome sequence, Nature 393 (1998) 537–544.
[11] E. Ellengand, C. Gerez, S. Un, M. Knüpling, G. Lu, J. Salem, H. Rubin, S. Sauge-Merle, J.P. Laulhère, M. Fontecave, Reactivity studies of the tyrosyl radical in ribonucleotide reductase from Mycobacterium tuberculosis and Arabidopsis thaliana. Comparison with *Escherichia coli* and mouse, Eur. J. Biochem. 258 (1998) 485–490.
[12] A. Liu, A.-L. Barra, H. Rubin, G. Lu, A. Gräslund, Heterogenity of the local electrostatic environment of the tyrosyl radical in *Mycobacterium tuberculosis* ribonucleotide reductase observed by high-field electron paramagnetic resonance, J. Am. Chem. Soc. 122 (2000) 1974–1978.
[13] A. Davydov, A. Liu, A. Gräslund, Heterogeneity of the ligand structure of the diferric site in *Mycobacterium tuberculosis* ribonucleotide reductase R2-2 protein, J. Inorg. Biochem. 80 (2000) 213–218.
[14] A. Ehrenberg, P. Reichard, Electron spin resonance of the iron-containing protein B2 from ribonucleotide reductase, J. Biol. Chem. 247 (1972) 3485–3488.
[15] A.J. Narváez, N. Voevodskaya, L. Thelander, A. Gräslund, The involvement of Arg265 of mouse ribonucleotide reductase R2 protein in proton transfer and catalysis, J. Biol. Chem. 281 (2006) 26022–26028.
[16] D. Lembo, G. Gribaudo, A. Hofer, L. Riera, M. Coriglia, A. Monro, A. Angeretti, M. Gariglio, L. Thelander, S. Landolfo, Expression of an altered ribonucleotide reductase activity associated with the replication of murine cytomegalovirus in quiescent fibroblasts, J. Virol. 74 (2000) 11557–11565.
[17] M.R. Seyedsayamdost, C.S. Yee, S.Y. Reece, D.G. Nocera, J. Stubbe, pH rate profiles of F_nY_{356}-R2s (n=2, 3, 4) in *Escherichia coli* ribonucleotide reductase: evidence that Y_{356} is a redox-active amino acid along the radical propagation pathway, J. Am. Chem. Soc. 128 (2006) 1562–1568.
[18] P. Nordlund, B-M. Sjöberg, H. Eklund, Three-dimensional structure of the free radical protein of ribonucleotide reductase, Nature 345 (1990) 593–598.
[19] M. Uppsten, J. Davis, H. Rubin, U. Uhlin, Crystal structure of the biologically active form of class Ib ribonucleotide reductase small subunit from Mycobacterium tuberculosis, FEBS Lett. 569 (2004) 117–122.
[20] A. Liu, S. Pötsch, A. Davydov, A.L. Barra, H. Rubin, A. Gräslund, The tyrosyl free radical of recombinant ribonucleotide reductase from Mycobacterium tuberculosis is located in a rigid hydrophobic pocket, Biochemistry 37 (1998) 16369–16377.
[21] G.J. Mann, A. Gräslund, E.I. Ochai, R. Ingemarson, L. Thelander, Purification and characterization of recombinant mouse and herpes simplex virus ribonucleotide reductase R2 subunit, Biochemistry 30 (1991) 1939–1947.
[22] A. Hofer, P.P. Schmidt, A. Gräslund, L. Thelander, Cloning and characterization of the R1 and R2 subunits of ribonucleotide reductase from *Trypanosoma brucei*, Proc. Natl. Acad. Sci. U.S.A. 94 (1997) 6959–6964.
[23] L. Whitmore, B.A. Wallace, DICHROWEB, an online server for protein secondary structure analyses from circular dichroism spectroscopy data, Nucleic Acids Res. 32 (2004) 668–673.
[24] A. Lobley, L. Whitmore, B.A. Wallace, DICHROWEB: an interactive web-site for the analysis of protein secondary structure from circular dichroism spectra, Bioinformatics 18 (2002) 211–212.
[25] N. Sreema, S.Yu. Venyaminov, R.W. Wood, Estimation of the number of α-helical and β-strand segments in proteins using circular dichroism spectroscopy, Protein Sci. 8 (1999) 370–380.
[26] www.ncbi.nlm.nih.gov/sites/entrez.
[27] www.ebi.ac.uk/Tools/amboss/align/index.html.
[28] mobyle.pasteur.fr.
[29] S.E. Radford, D.N. Woolfson, S.R. Martin, G. Lowe, C.M. Dobson, A three-disulphide derivative of hen lysozyme. Structure, dynamics and stability, Biochem. J. 273 (1991) 211–217.
[30] M. Mizuguchi, K. Masaki, K. Nitta, The molten globule state of a chimera of human alpha-lactalbumin and equine lysozyme, J. Mol. Biol. 292 (1999) 1137–1148.
[31] A.A. Moosavi-Movahedi, J. Chamani, Y. Goto, G.H. Hakimelahi, Formation of the molten globule-like state of cytochrome *c* induced by *n*-alkyl sulfates at low concentrations, J. Biochem. 133 (2003) 93–102.
[32] R. Mohana-Bordes, N.K. Goto, G.J. Kroon, H.J. Dyson, P.E. Wright, Structural characterization of unfolded states of apomyoglobin using residual dipolar couplings, J. Mol. Biol. 340 (2004) 1131–1142.
[33] O.S. Makin, L.C. Serpell, Structures for amyloid fibrils, FEBS J. 272 (2005) 5950–5961.
[34] J. Danielsson, J. Jarvet, P. Damberg, A. Gräslund, Translational diffusion measured by PFG-NMR on full length and fragments of the Alzheimer Aβ(1–40) peptide. Determination of hydrodynamic radii of random coil peptides of varying length, Magn. Res. Chem. 40 (2004) S89–S97.
[35] D.K. Wilkins, S.B. Grimshaw, V. Receveur, C.M. Dobson, J.A. Jones, L.J. Smith, Hydrodynamic radii of native and denaturated proteins measured by pulse field gradient NMR techniques, Biochemistry 38 (1999) 16424–16431.
[36] H. Uchiyama, E.M. Perez-Prat, K. Watanabe, I. Kumagai, K. Kuwajima, Effects of amino acid substitutions in the hydrophobic core of alpha-lactalbumin on the stability of the molten globule state, Protein Eng. 8 (1995) 1153–1161.
[37] M. Meyer-Luehmann, M. Stalder, M.C. Herzig, S.A. Kaeser, E. Kohler, M. Pfeifer, S. Boncristino, P.M. Mathews, M. Mercken, D. Abramowski, M. Jucker, Extracellular amyloid formation and associated pathology in neural grafts, Nat. Neurosci. 6 (2003) 370–377.
[38] R. Kayed, E. Head, J.L. Thompson, T.M. McIntire, S.C. Milton, C.W. Cotman, C.G. Glabe, Common structure of soluble amyloid oligomers implies common mechanism of pathogenesis, Science 300 (2003) 486–489.
[39] A. Päiviö, J. Jarvet, A. Gräslund, L. Lannfelt, A. Westlind-Danielsson, Unique physicochemical profile of β-amyloid peptide variant Aβ1-40E22G protofibrils: conceivable neuropathogen in arctic mutant carriers, J.Mol. Biol. 339 (2004) 145–159.
[40] B. Caughey, Transmissible spongiform encephalopathies, amyloidoses and yeast prions: common threads? Nat. Med. 6 (2000) 751–754.
[41] J.W.M. Höppener, M.G. Nieuwenhuis, T.M. Vroom, B. Ahrén, C.J.M. Lips, Role of islet amyloid in type 2 diabetes mellitus: consequence or cause? Mol. Cell. Endocrin. 197 (2002) 205–212.